Atmospheric Environment 213 (2019) 585–596

Contents lists available at ScienceDirect

Atmospheric Environment

journal homepage: www.elsevier.com/locate/atmosenv

Soil organic carbon and nutrient losses resulted from spring dust emissions in Northern China

Hongquan Song[a,b,1], Kesheng Zhang[a,1], Shilong Piao[c], Lingli Liu[d], Ying-Ping Wang[e], Youmin Chen[b], Zhongling Yang[a], Lili Zhu[a], Shiqiang Wan[a,f,*]

[a] International Joint Research Laboratory for Global Change Ecology, State Key Laboratory of Cotton Biology, School of Life Sciences, Henan University, Kaifeng, Henan, 475004, China

[b] Key Laboratory of Geospatial Technology for the Middle and Lower Yellow River Regions, Ministry of Education, College of Environment and Planning, Henan University, Kaifeng, Henan, 475004, China

[c] Sino-French Institute for Earth System Science, College of Urban and Environmental Sciences, Peking University, Beijing, 100871, China

[d] State Key Laboratory of Vegetation and Environmental Change, Institute of Botany, Chinese Academy of Sciences, Xiangshan, Beijing, 100093, China

[e] CSIRO Ocean and Atmosphere Flagship, PMB 1, Aspendale, Vic. 3195, Australia

[f] College of Life Sciences, Hebei University, Baoding, Hebei, 071000, China

GRAPHICAL ABSTRACT

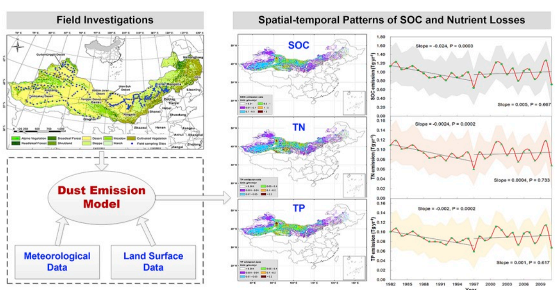

ARTICLE INFO

Keywords:
Wind erosion
Spatial-temporal patterns
Soil organic carbon losses
Nitrogen losses
Phosphorus losses

ABSTRACT

Dust emissions due to wind erosion have significant impacts on air quality, climate, and biogeochemical processes. Arid and semi-arid regions in Northern China are a major contributor to global dust emissions. However, how dust emissions affect soil organic carbon (SOC) and nutrient losses in this region are poorly understood. In this study, we estimated the spatial patterns and temporal dynamics of SOC and nutrient (total nitrogen (TN) and total phosphorus (TP)) losses in spring using a process-based dust emission model in Northern China during 1982–2011. Spatial patterns of SOC and nutrient losses are consistent with dust emission rates across the research region. Annual losses of SOC, TN, and TP resulted from wind erosion in spring were $0.985 \pm 0.149\ \mathrm{Tg\ yr^{-1}}$, $0.094 \pm 0.014\ \mathrm{Tg\ yr^{-1}}$, and $0.089 \pm 0.013\ \mathrm{Tg\ yr^{-1}}$, respectively. Two distinct periods with opposite trends were identified in dust emissions and SOC and nutrient losses, declining from 1982 to 1997 and then increasing. The opposite patterns in Northern China are largely attributed to the changes in vegetation growth due to climate change and shifts of green-up date of vegetation. The findings could help to reduce the uncertainties in simulating regional biogeochemical cycling in Northern China.

* Corresponding author. School of Life Sciences, Henan University Jinming Campus, Kaifeng, Henan Province 475004, China.
E-mail address: swan@hbu.edu.cn (S. Wan).

[1] These authors contributed equally to this work and should be considered co-first authors.

https://doi.org/10.1016/j.atmosenv.2019.06.043
Received 23 October 2018; Received in revised form 23 May 2019; Accepted 22 June 2019
Available online 27 June 2019
1352-2310/

1. Introduction

The dust emission, transport, and deposition can influence terrestrial nutrients cycling (Reynolds et al., 2001), ocean productivity (Jickells et al., 2005), air quality (Monks et al., 2009; Li et al., 2019), human health (Griffin, 2007; Lelieveld et al., 2015), and regional to global climate (Tegen et al., 1996; Evan et al., 2016; Song et al., 2017). The annual global dust emission caused by wind erosion ranges from 500 to 4300 Mt (Huneeus et al., 2011). The area affected by wind erosion in China is approximately 1.91 million km^2, accounting for 20% of the national territory (Wang et al., 2006), which is a primary contributor to atmospheric dust aerosols in East Asia (Song et al., 2016) and frequently transported over long distances to North Pacific Ocean, North America (Yu et al., 2012), and even Europe (Grousset et al., 2003). Soil organic carbon (SOC) and nutrient losses associated with wind erosion and dust emissions in this region can profoundly impact plant growth and productivity as well as ecosystem carbon (C) cycling and sequestration in China.

Dust emissions can remove considerable quantities of top soils enriched with SOC and nutrients from the source area (Harper et al., 2010), which is a major process of soil degradation in arid and semi-arid regions (Van Oost et al., 2007; Chappell et al., 2019). SOC and nutrients associated with fine soil particles can be transported hundreds and thousands of kilometers and influence ecosystems far away from the source regions (Webb et al., 2012). Numerous studies have been conducted to investigate the impacts of dust emissions on SOC and nutrient losses over the past several decades, including field experiments (Wang et al., 2006; Hoffmann et al., 2011), remote sensing (Yan et al., 2005; Yu et al., 2015), model simulations (Chappell et al., 2013, 2019), and ^{137}Cs analysis (Chappell et al., 2014). However, these studies mainly concentrated on the SOC losses and large uncertainties remain. For example, the annual SOC emission in China can vary from 3 $Tg\,yr^{-1}$ (Duan et al., 1996) to 75 $Tg\,yr^{-1}$ (Yan et al., 2005). In a review study, Wang et al. (2006) estimated the annual soil C and nitrogen (N) losses due to wind erosion ranging from 59 to 4514 $kg\,C\,ha^{-1}$ and from 5.9 to 387 $kg\,N\,ha^{-1}$, respectively.

The severity of wind erosion is generally controlled by the threshold friction velocity (u_{*t}) associated with the wind speed, precipitation, soil composition, soil moisture, and vegetation (Liu et al., 2004; Cowie et al., 2013; Kim and Choi, 2015). Surface friction wind velocities (u_*) can be inhibited or stimulated due to the changes of surface roughness induced by increased or decreased vegetation cover (Cao et al., 2011). The vegetation growth is sensitive to climatic change in boreal and temperate regions over the past several decades (Piao et al., 2008). Climate change in Northern China leads to substantial difference in plant growth and vegetation cover, resulting in great variability in spatial patterns and temporal trends of SOC and nutrient losses due to wind erosion over the past several decades. In addition, land use may play an important role in regulating dust emissions, particularly in the Northeast and the Southern margin of the Loess Plateau (Ginoux and Deroubaix, 2017).

Most of the previous studies mainly focus on wind erosion impacts on the losses of SOC and/or N. Phosphorus (P) can also limit plant productivity and C storage in terrestrial ecosystems (Katra et al., 2016). However, little research efforts have been made to investigate losses of soil P due to wind erosion. Thus, a comprehensive quantification of

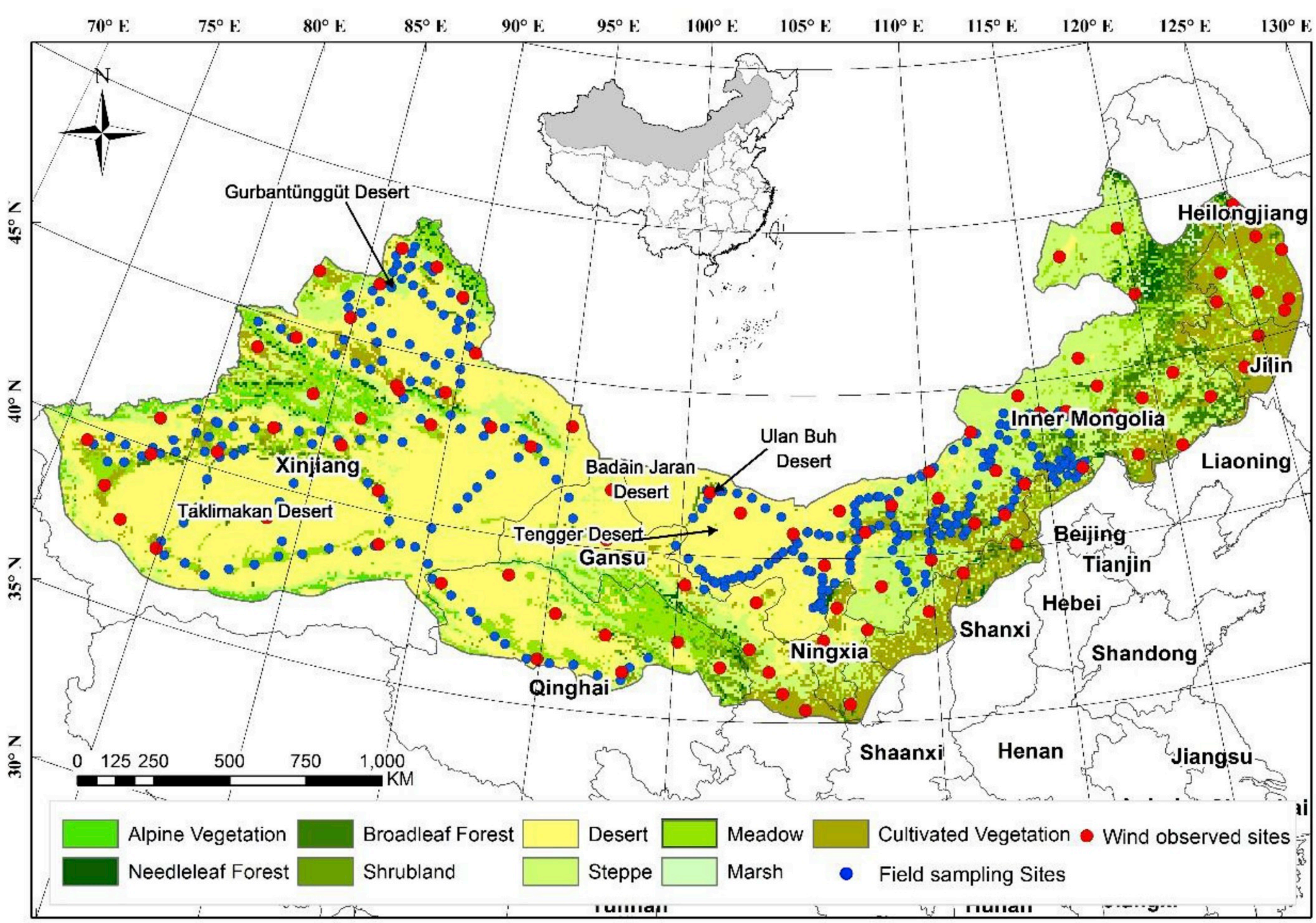

Fig. 1. Spatial distributions of vegetation types, field sampling sites (blue circles), and meteorological stations (red circles) in Northern China. (For interpretation of the references to colour in this figure legend, the reader is referred to the Web version of this article.)

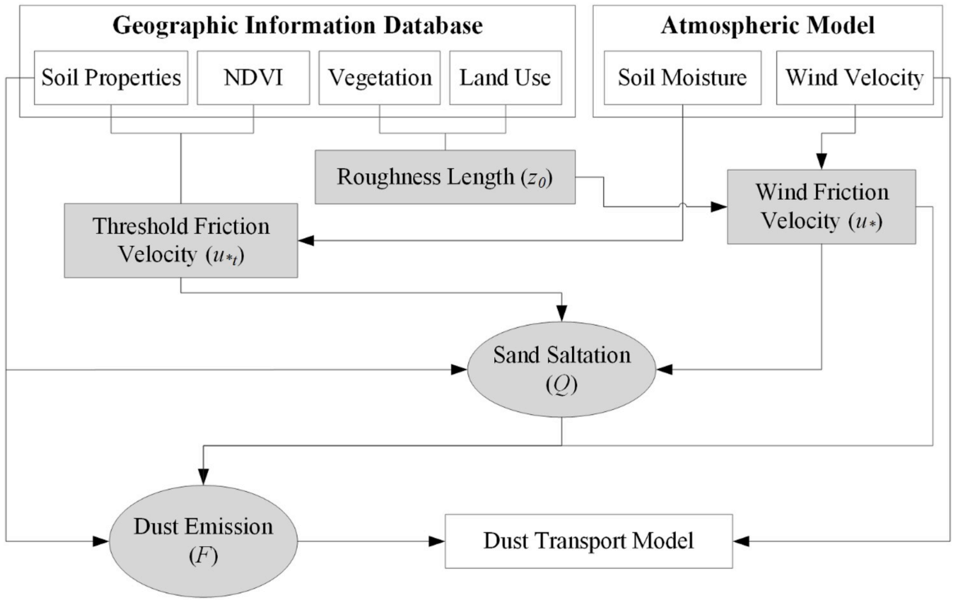

Fig. 2. The structure of the wind erosion scheme.

SOC, N, and P losses induced by wind erosion is critical to understand the relationships of SOC and nutrient budgets with dust emissions and the consequent impacts on plant growth and productivity.

This study evaluated the dust emission model using datasets from field investigations that mimicked the wind erosion and simulated the spatial patterns and temporal dynamics in losses of SOC, N, and P under wind erosion over Northern China during the spring of 1982–2011.

2. Materials and methods

2.1. Research region and field samplings

The study area is the arid and semi-arid regions of Northern China with temperate continental climate (Fig. 1). Deserts and temperate steppes are the major vegetation types in this region. The total area accounts for approximately 30% of the China territory with mean annual precipitation less than 400 mm and annual mean temperature ranging from 0 °C to 13 °C.

To evaluate the performance of dust emission simulations and the accuracy of SOC and nutrient datasets in Northern China, field investigations mimicking dust emission were conducted in the spring (March–May) of 2014 and 2015. Three 1 × 1 m plots were selected at each sampling site (Fig. S1). We collected soil particles, which have been uplifted by blowing winds generated by a pneumatic extinguisher at a specific wind velocity for each plot (Fig. S1b). To reduce the turbulences generated by the pneumatic extinguisher and make it similar to natural wind, we redesigned it by increasing the length and the cross-sectional area of the airflow outlet (Fig. S1b). The uplifted dust weight was measured after removed plant litters in the collected samples for each plot. Parameters required for the dust emission model and the estimation of SOC and nutrient losses were measured in the top soils (0–10 cm), including vegetation cover, soil moisture, bulk density, particles diameter distribution, and contents of SOC and N. Field samplings were conducted at 293 sites (Fig. 1) across the research region, which were utilized to evaluate the performance of the dust emission model and contents of SOC and nutrient datasets.

2.2. Dust emission model description

The dust emission simulation was the rudimentary procedure for the estimation of SOC and nutrient losses. In this study, we adopted a wind erosion scheme, which is a component of the Integrated Wind Erosion Modeling System (IWEMS; Lu and Shao, 2001) to simulate the spatial-temporal variations of spring dust emissions during 1982–2011 in Northern China. IWEMS is a process-based model developed by Lu and Shao (2001), and consists of an atmospheric model, a land surface model, a wind erosion scheme, a dust transport and deposition scheme, and a geographic information database. The atmospheric model provides wind velocity and eddy diffusivity data, which are used to drive wind erosion and transport model. To simulate dust emission rate, meteorological and land surface data are passed to the wind erosion scheme at each physical time step. The geographic information database provides spatial distributions of land surface data for the dust emission model, such as soil properties, friction velocity, etc. Dust emissions and atmospheric data are then passed to the dust transport model to predict the dust motion (Shao et al., 2003). Numerous studies have been adopted the IWEMS to simulate dust emissions over East Asia (Shao et al., 2002; Mao et al., 2011, 2013; Du et al., 2014; Song et al., 2016, 2017) and demonstrated that it had good performance in the simulation for dust emissions over East Asia, especially in gobi desert areas (Su and Fung, 2015).

In this study, we concentrated on the dust emission for the estimation of SOC and nutrient losses rather than its transport and deposition. Therefore, the component of the wind erosion scheme in IWEMS was adopted to simulate dust emissions in Northern China. The wind speed was used as the wind erosion scheme's input without including the wind direction. Fig. 2 shows the structure of the wind erosion scheme. Three mandatory parameters should be represented in this wind erosion model, including the erosion threshold friction velocity u_{*t}, the streamwise saltation flux Q, and the dust emission rate F for each size classes of dust particles.

The threshold friction velocity for particle-size d_s can be calculated using a simple equation

$$u_{*t}(d_s) = \sqrt{a_1\left(\frac{\rho_p}{\rho_a}gd_s + \frac{a_2}{\rho_a d_s}\right)} \quad (1)$$

where ρ_a is the air density, ρ_p is the density of sand particles, g is the acceleration of gravity, a_1 is a dimensionless parameter (0.0123), a_2 is a dimensioning parameter ($3 \times 10^{-4}\,\mathrm{kg\,s^{-2}}$), d_s is the sand particle diameter. The threshold friction velocity with roughness elements (Raupach et al., 1993) can be calculated as

$$u_{*t}(d_s, \lambda) = u_{*t}(d_s)\sqrt{(1 - m_\gamma \sigma_\gamma \gamma)(1 + m_\gamma \beta_\gamma \lambda)} \quad (2)$$

where m_γ is a tuning parameter with a value less than one which accounts for non-uniformities in the surface stress distribution ($m_\gamma \approx 0.5$), σ_γ is the ratio of basal area to the frontal area ($\sigma_\gamma \approx 1$), β_γ is the ratio of the pressure-drag coefficient to the friction drag coefficient ($\beta_\gamma \approx 90$), λ is the frontal area index of the roughness element. The frontal area index required for the calculation of threshold friction velocity is estimated from NDVI (Lu and Shao, 2001).

The horizontal saltation flux, Q, is calculated by the theoretical equation proposed by Owen (1964). For uniform sand particle soil, the horizontal sediment flux is calculated as

$$\tilde{Q} = \begin{cases} \left(\frac{c\rho_a u_*^3}{g}\right)\left[1 - \left(\frac{u_{*t}(d)}{u_*}\right)^2\right] & u_* \geq u_{*t}(d) \\ 0 & u_* < u_{*t}(d) \end{cases} \quad (3)$$

where c is Owen's coefficient, u_* is the friction velocity, and u_{*t} (d) is threshold friction velocity for particles with the diameter of d. For the calculation method of u_{*t} (d), please refer to Lu and Shao (2001). The total horizontal dust flux can be estimated by a weighted integral of $\tilde{Q}(d)$ over each size class defined by the particle size distribution $p(d)$:

$$Q = \int \tilde{Q}(d)p(d)\delta d \quad (4)$$

Four dust particle size groups, including $d \leq 2\,\mu m$ (clay), $2 < d \leq 11\,\mu m$ (fine silt), $11 < d \leq 22\,\mu m$ (medium silt), and $22 < d \leq 52\,\mu m$ (large silt), are considered in this study (Lu and Shao, 2001). The dust emission rate (vertical dust flux), F, is calculated by the wind erosion scheme in the IWEMS developed by Lu and Shao (1999):

$$F = \frac{C_\alpha g f \rho_b}{2p}\left(0.24 + C_\beta u_* \sqrt{\frac{\rho_p}{p}}\right)Q \quad (5)$$

where Q is the horizontal saltation flux, f is the total volumetric fraction of dust in the sediment, ρ_b is the bulk soil density, ρ_p is the particle density, p is the soil plastic pressure exerted by soil on a particle moving through it, C_α and C_β are coefficients of order 1. An integration of Eq. (5) over the particle size range gives the total vertical dust flux from the soil surface for a given u_*. The plastic pressure, p, is $> 10^5\,N\,m^{-2}$ (Lu and Shao, 1999) for most natural soils. This allows a further simplification of Eq. (5) to

$$F = \frac{0.12 C_\alpha g f \rho_b}{p} Q \quad (6)$$

which is used in this study. For details of the vertical dust flux calculation, please refer to the literature of Lu and Shao (2001).

2.3. Datasets

Land surface variables required by the dust emission model are soil properties, vegetation cover, and land use. Soil variables were obtained from the Harmonized World Soil Database (HWSD). The soil map of China in HWSD with a map scale of 1:1,000,000 was based on data of the office for the Second National Soil Survey of China (1995) and distributed by the Institute of Soil Science in Nanjing (Shi et al., 2004), which was utilized to create map layers of soil types, bulk density, clay fraction, etc. The vegetation cover was derived based on the third generation of Normalized Deviation Vegetation Index (NDVI3g) from Global Inventory Modeling and Mapping Studies (GIMMS) during 1982–2011 (Tucker et al., 2005). The spatial resolution of this dataset is 1/12-degree and the temporal resolution is half month. Land use map layers with a map scale of 1:100,000 in 1980s, 1995, and 2000 had 25 categories were obtained from Data Sharing Infrastructure of Earth System Science and were integrated with soil data to extract the erodible fraction based on the methods proposed by Lu and Shao (2001).

Three types of wind field datasets, including National Centers for Environmental Prediction and National Center for Atmospheric Research (NCEP) reanalysis datasets, European Center for Medium-Range Weather Forecasts (ECMWF), and China Meteorological Forcing Dataset (CMFD) were adopted to force the wind erosion model from 1982 to 2011. Datasets of NCEP reanalysis and ECMWF were updated every 6 h, and the spatial resolutions of them were $2.5^\circ \times 2.5^\circ$ and $0.25^\circ \times 0.25^\circ$, respectively. The CMFD, however, was updated every 3 h with a spatial resolution of $0.1^\circ \times 0.1^\circ$, which was developed by Data Assimilation and Modeling Center for Tibetan Multi-spheres, Institute of Tibetan Plateau Research, Chinese Academy of Sciences (He and Yang, 2011). Observed wind speed, temperature, and precipitation at 91 sites across the research region (Fig. 1) were obtained from NOAA-National Climatic Data Center Surface (NCDC), which were used to evaluate the accuracy of the three wind speed datasets and analyze the climate during the research period.

To estimate SOC and nutrient losses, spatial distributions of SOC, N, and P contents obtained from Soil Database of China for Land Surface Modeling (SDCLSM) were used to quantify SOC and nutrient losses due to wind erosion. SDCLSM has a spatial resolution of 30 × 30 arc-seconds which was derived from 8979 soil profiles and the Soil Map of China (1:1,000,000) (Shangguan et al., 2013). The soil organic matter (SOM) content of SDCLSM were converted to organic carbon contents using the factor 0.58 (guidelines in the National Soil Survey Handbook, http://soils.usda.gov/technical/handbook).

2.4. Model evaluation and simulation

It is challenging to conduct a comprehensive evaluation of the performance for the dust emission model because of limited field observations on dust emissions in China. With the assumption that dust emissions are closely associated with the dust storm frequency, we have evaluated this wind erosion model using dust storm frequency datasets from the meteorological network of China Meteorological Data Center in Fig. 7 by Song et al. (2016). The simulated dust emissions during that study period were well correlated with observed dust storm frequencies (Song et al., 2016).

The accuracy of wind speeds is crucial to the dust emission simulation due to it is the main driver of wind erosion. Large variances exist in the three wind speed datasets adopted in this study (Fig. 3a, b, and c), although the correlations between NCEP ($R = 0.327$, $P < 0.001$), CMFD ($R = 0.809$, $P < 0.001$), and ECMWF ($R = 0.511$, $P < 0.001$) and observed wind speeds were significant over the research region. This could result in different dust emissions between simulations by the three wind speed datasets. In this study, the wind erosion model was driven by the measured data from the mimicking wind erosion at 293 sites (blue circles in Fig. 1), and then the simulations were compared with the measured dust emissions (Fig. 3d). Results showed that model simulations fitted well ($R = 0.80$, $P < 0.001$) with the field sampling (Figs. 3d and S2).

To evaluate the SOM and nutrient contents in soil inventories, comparisons were made between their contents in soil datasets and the measured SOC and TN contents. However, TP contents were not measured for the soil samples in the field investigations. The SOM in SDCLSM was well correlated with measured SOC contents ($R = 0.642$, $P < 0.001$) (Fig. 3e), and the spatial pattern of measured SOC was consistent with the spatial distribution of SOC in the soil datasets (Fig. S3a). The TN contents in soil datasets were positively correlated with the measured contents ($R = 0.472$, $P < 0.001$) (Fig. 3f). The TN contents in SDCLSM may be underestimated to some extent. In addition, the spatial pattern of the measured TN contents in the research region was well consistent with the spatial distributions of TN contents in SDCLSM (Fig. S3b). The mimicked dust emissions demonstrated that dust emissions mainly occurred in regions of low vegetation cover (Fig. 4).

Dust emissions in Northern China were simulated over 3 months (March 1 to May 31) in each year from 1982 to 2011 forced by

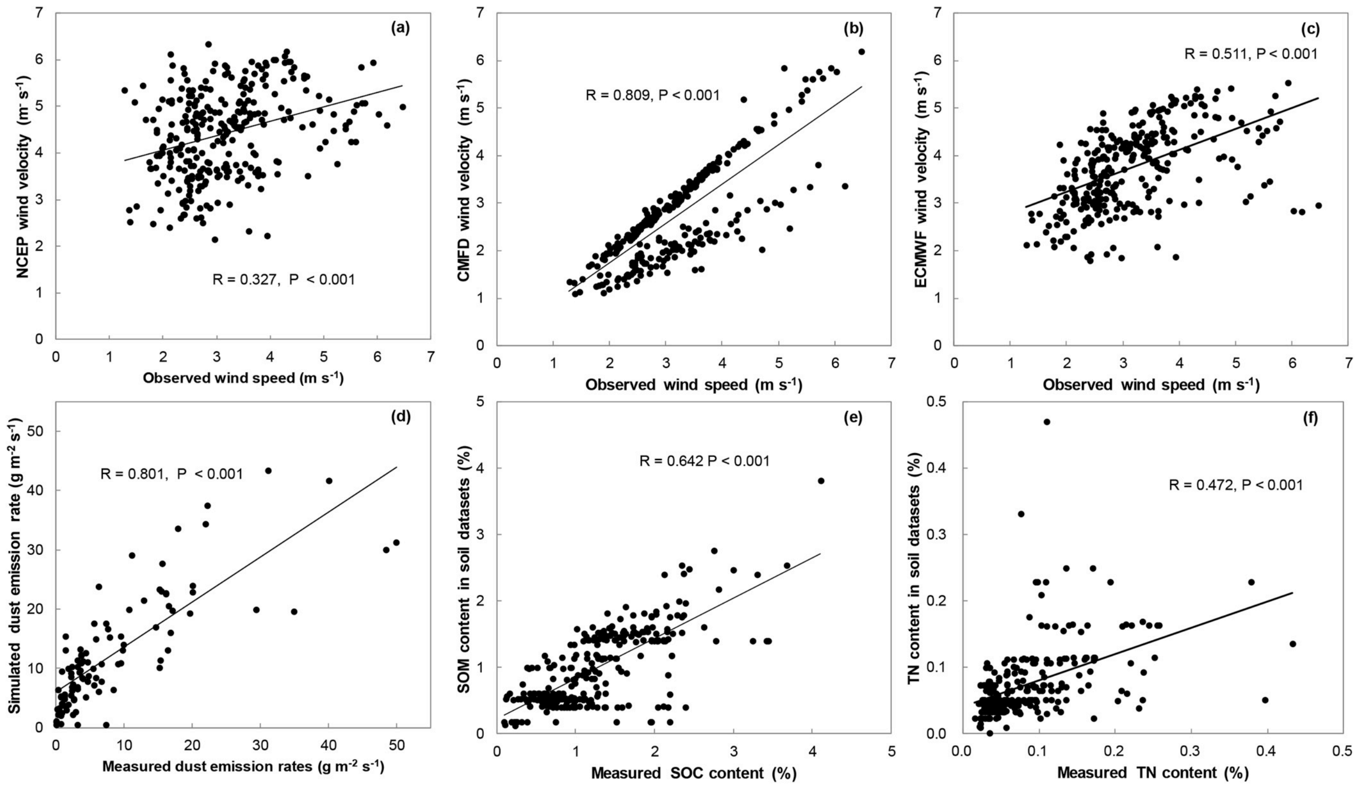

Fig. 3. Relationships of the simulated wind speeds (a, NCEP; b, CMFD; c, ECMWF) with observed wind speeds, of the simulated dust emission rates with the measured dust emission rates (d), and of SOC (e) and TN (f) contents in soil datasets of SDCLSM with SOC and TN contents measured in field investigations.

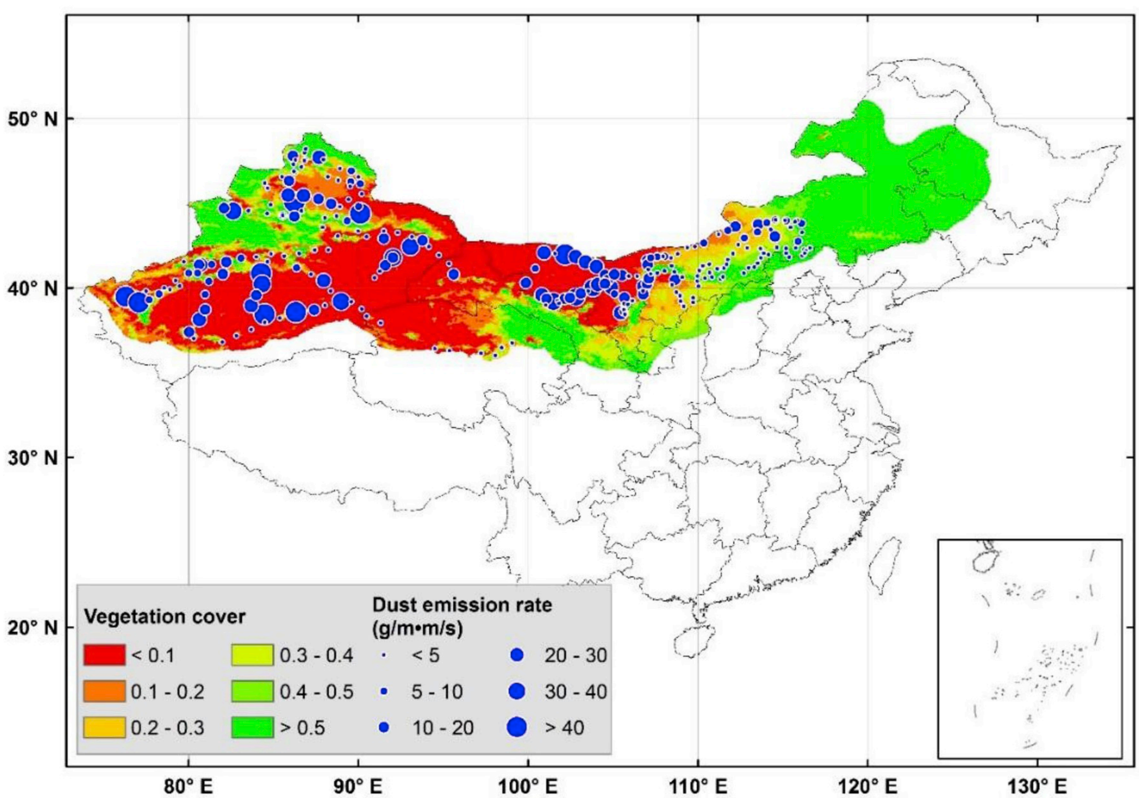

Fig. 4. The map of mimicked dust emissions (blue circles) and vegetation cover. (For interpretation of the references to colour in this figure legend, the reader is referred to the Web version of this article.)

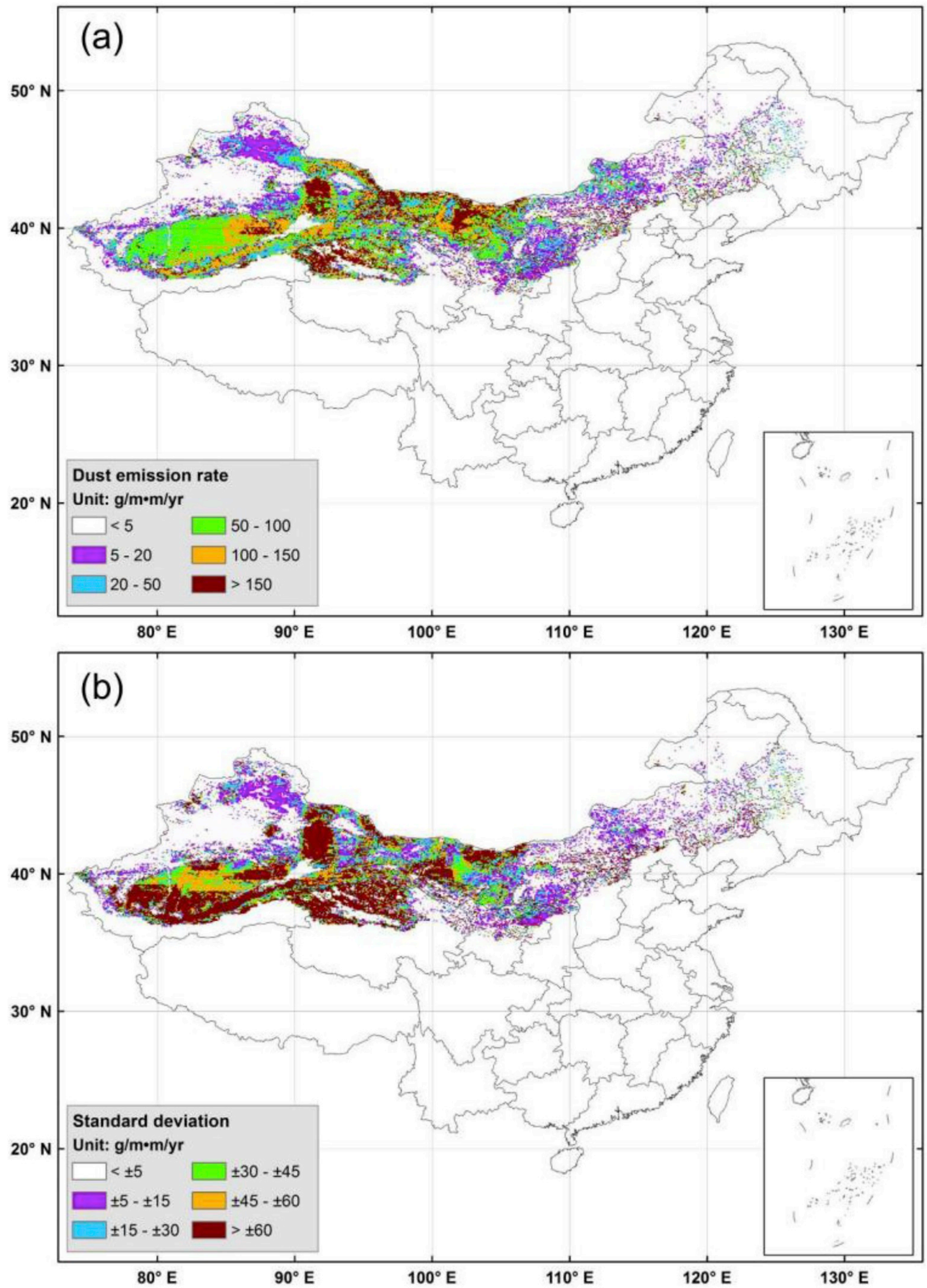

Fig. 5. Spatial distributions of annual averages of spring (March–May) dust emission rates (a) and the standard deviations of averaged simulations parameterized by NCEP, ECMWF, and CMFD (b).

meteorological fields and land surface inventories. All datasets were projected to the same spatial coordinate system through the Albers map projection and re-gridded to the horizontal resolution of 8 km × 8 km before simulations. The dust parameterization is driven by three to six-hourly meteorological fields, annual vegetation cover, decadal (e.g. land use) or fixed (e.g. soil) surface properties. Losses of SOC, N, and P, in this study, were estimated through multiplying the dust emission amount by the contents of SOC, N, and P in Northern China using the method proposed by Yan et al. (2005).

3. Results

3.1. Spatial and temporal variations of dust emissions

The average of simulated spring dust emissions (Fig. 5a) showed that the wind erosion mainly occurred in the deserts of arid and semi-arid areas (Fig. 1) in Northern China. The vegetation cover was lower than 0.2 (Fig. 4) and the annual spring dust emission rates were greater than $50\ g\ m^{-2}\ yr^{-1}$ (Fig. 5a) across the intensified wind erosion regions. The largest standard deviations ($> \pm 60\ g\ m^{-2}\ yr^{-1}$) of averaged dust emissions simulated by the three wind datasets distributed in regions of Southern Taklimakan Desert, Eastern Xinjiang, Northern

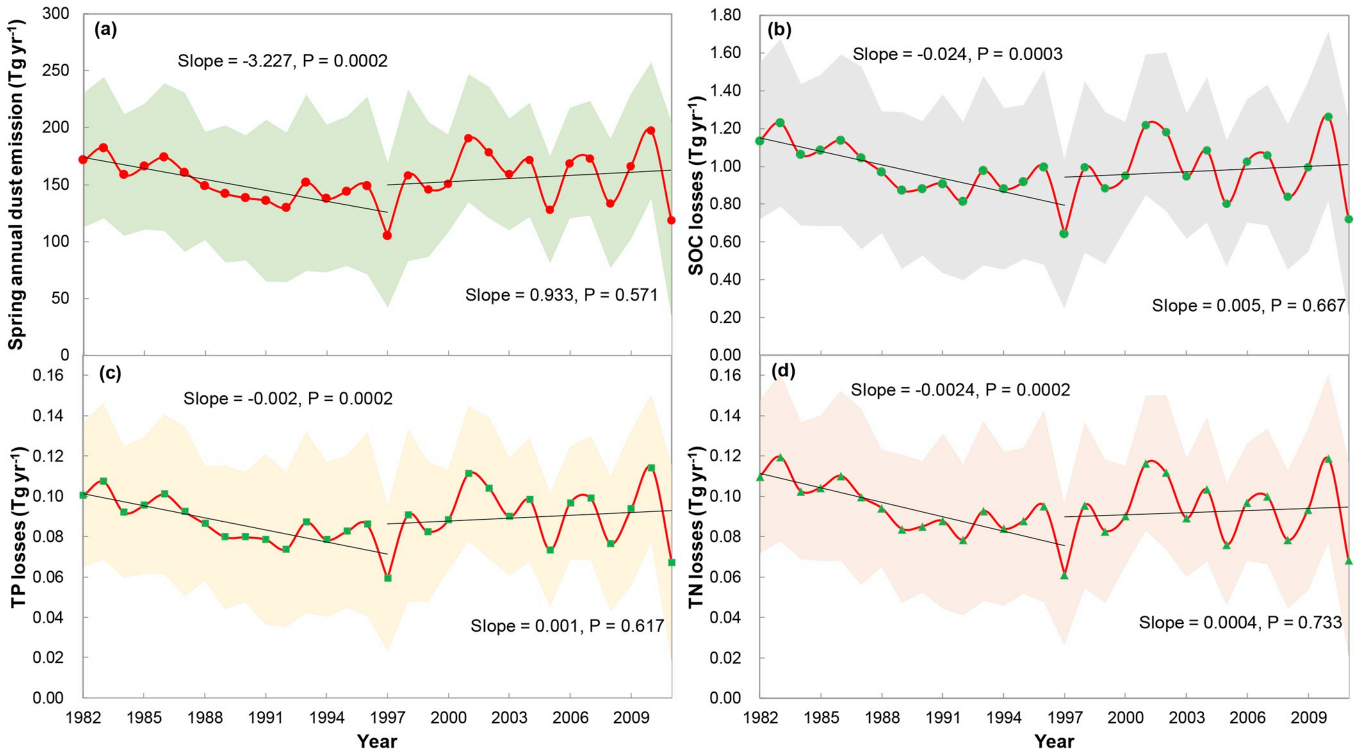

Fig. 6. Inter-annual variations of dust emissions (a) and annual losses of SOC (b), TN (c), and TP (d) during periods of 1982–1997 and 1997–2011 at the regional scale and shaded areas denoted standard deviations of averaged dust emission (a) and losses of SOC (b), TN (c), and TP (d) losses simulated by three wind field datasets (CMFD, ECMWF, and NCEP).

Qinghai, and parts of Inner Mongolia (Fig. 5b).

The average of spring dust emissions was 154.45 ± 21.28 Tg yr^{-1} (Fig. 6a) and the annual spring dust emissions simulated by NCEP, ECMWF, and CMFD were 220.11 ± 20.3 Tg yr^{-1}, 110.24 ± 14.8 Tg yr^{-1}, and 132.98 ± 38.3 Tg yr^{-1}, respectively (Fig. S4). The difference between the two simulations by NCEP and ECMWF can reach a factor of 2 and the simulation of CMFD had the largest fluctuations (Fig. S4). This may be due to the overall simulated NCEP was higher than the simulated ECMWF (Fig. 2a and c). The maximum and minimum annual spring dust emissions for 1982–2011 were 197.47 ± 59.79 Tg yr^{-1} in 2010 and 105.20 ± 63.22 Tg yr^{-1} in 1997 (Fig. 6a). Although a general declining trend of dust emissions is simulated over the entire study period, there were two clearly distinct periods with opposite trends before and after 1997 (Fig. 6a). The annual spring dust emissions generally decreased by −3.227 Tg yr^{-1} ($P < 0.001$) between 1982 and 1997, but slightly increased by 0.933 Tg yr^{-1} ($P = 0.571$) since 1997 (Fig. 6a).

3.2. Temporal changes in losses of SOC and nutrient

At the regional scale, the annual losses of SOC (Fig. 6b), TN (Fig. 6c), and TP (Fig. 6d) during spring due to wind erosion were 0.985 ± 0.149 Tg yr^{-1}, 0.094 ± 0.014 Tg yr^{-1}, and 0.089 ± 0.013 Tg yr^{-1}, respectively. The maximum losses of SOC (1.266 ± 0.449 Tg yr^{-1}), TN (0.119 ± 0.042 Tg yr^{-1}), and TP (0.114 ± 0.037 Tg yr^{-1}) appeared in 2010 and the minimum losses of SOC (0.644 ± 0.393 Tg yr^{-1}), TN (0.061 ± 0.035 Tg yr^{-1}), and TP (0.059 ± 0.036 Tg yr^{-1}) occurred in 1997 (Fig. 6b, c, and d). There were substantial discrepancies in the losses of SOC and nutrient simulated by ECMWF (SOC, 0.645 ± 0.101 Tg yr^{-1}; TN, 0.063 ± 0.010 Tg yr^{-1}; TP, 0.062 ± 0.009 Tg yr^{-1}), NCEP (SOC, 1.471 ± 0.164 Tg yr^{-1}; TN, 0.139 ± 0.016 Tg yr^{-1}; TP, 0.128 ± 0.013 Tg yr^{-1}), and CMFD (SOC, 0.838 ± 0.248 Tg yr^{-1}; TN, 0.080 ± 0.023 Tg yr^{-1}; TP, 0.077 ± 0.023 Tg yr^{-1}) (Fig. S5).

Temporal trends in SOC (Fig. 6b), TN (Fig. 6c), and TP (Fig. 6d) losses were well consistent with the trends of dust emissions from 1982 to 2011 (Fig. 6a). Similar to the trends of dust emissions during the entire study period, two distinct opposite trends of SOC and nutrient losses before and after 1997 were identified. Averaged SOC losses in spring across Northern China decreased by −0.024 Tg yr^{-1} ($P < 0.001$) and then slightly increased by 0.005 Tg yr^{-1} ($P = 0.667$) before and after 1997, respectively (Fig. 6b). SOC losses declined by −0.016 Tg yr^{-1} ($P = 0.069$), −0.050 Tg yr^{-1} ($P < 0.001$), and −0.006 Tg yr^{-1} ($P = 0.193$) from 1982 to 1997 estimated by wind datasets of NCEP, CMFD, and ECMWF (Fig. S5a), respectively.

The averaged TN (Fig. 6c) and TP (Fig. 6d) losses in spring declined by −0.0024 Tg yr^{-1} ($P < 0.001$) and −0.002 Tg yr-1 ($P < 0.001$) before 1997 and then slightly elevated by 0.0004 Tg yr^{-1} ($P = 0.733$) and 0.001 Tg yr^{-1} ($P = 0.617$). The TN losses simulated by the three wind datasets (Fig. S5b) decreased by −0.0017 Tg yr^{-1} (NCEP, $P = 0.041$), −0.0049 Tg yr^{-1} (CMFD, $P < 0.001$), and −0.0006 Tg yr^{-1} (ECMWF, $P = 0.165$) from 1982 to 1997, but marginally raised at rates of 0.0011 Tg yr^{-1} (NCEP, $P = 0.349$) and 0.0004 Tg yr^{-1} (ECMWF, $P = 0.559$) from 1997 to 2011. During the period 1982–1997, TP losses decreased by −0.0013 Tg yr^{-1} (NCEP, $P = 0.057$), −0.0042 Tg yr^{-1} (CMFD, $P < 0.001$), and −0.0005 Tg yr^{-1} (ECMWF, $P = 0.203$) (Fig. S5c).

3.3. Spatial distributions of SOC and nutrient losses

The SOC contents in surface soils generally increased with increasing latitude in the east part and decreased from east to west in most areas of Northern China (Fig. S3a). Dust emissions mainly occurred in areas with low SOC content in the top soils (Figs. 5a and 7a). The annual SOC loss rate in spring was less than 3 g m^{-2} yr^{-1} across most regions (Fig. 7a). Areas with severe SOC losses were Western Inner Mongolia, Western Gansu, Northwestern Qinghai, and Eastern Xinjiang (Fig. 7a).

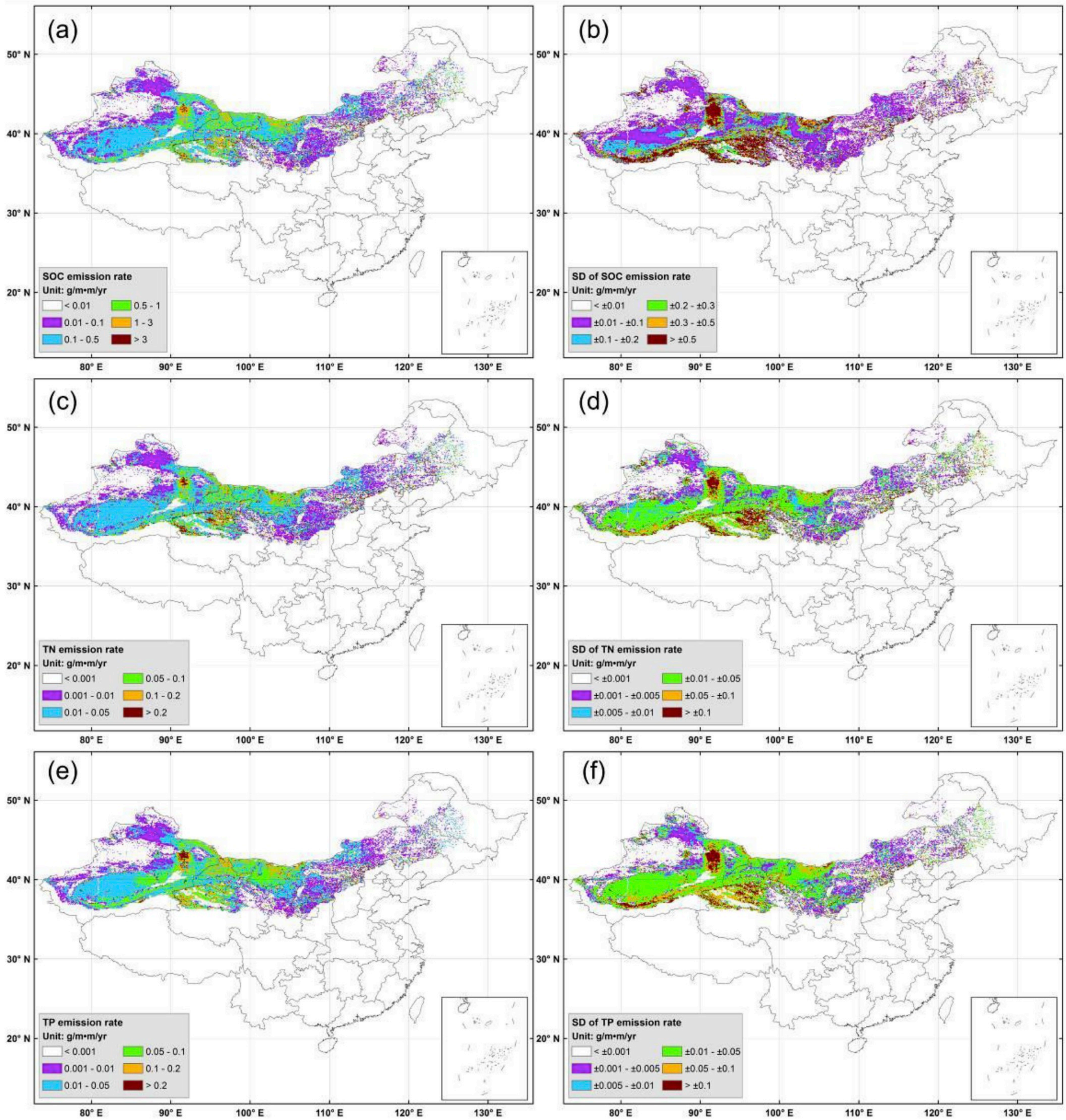

Fig. 7. Spatial distributions of annual averages of SOC (a), TN (c), and TP (e) losses and the standard deviations of averaged SOC (b), TN (d), and TP (f) losses simulated by the three wind field datasets (ECMWF, NCEP, and CMFD).

Both TN and TP contents in the top soils was less than 0.1% across most wind erosion areas in Northern China (Figs. S3b and c). Spring TN and TP losses in most areas of Northern China were less than 0.1 $g\,m^{-2}\,yr^{-1}$ (Fig. 7c and e) over the past three decades. Areas with severe TN and TP losses (> 0.1 $g\,m^{-2}\,yr^{-1}$) were in Eastern Xinjiang, Northwestern Gansu, Western Inner Mongolia, and parts of Northern Qinghai (Fig. 7c and e). Spatial patterns of SOC, TN and TP losses were heterogeneous in Northern China (Fig. 7a, c, and e). The largest standard deviations of averaged SOC (> $\pm$ 0.5 $g\,m^{-2}\,yr^{-1}$) and nutrient (> $\pm$ 0.1 $g\,m^{-2}\,yr^{-1}$) losses simulated by the three wind fields occurred in parts of Eastern Xinjiang and Northern Gansu (Fig. 7b, d, and f).

4. Discussion

4.1. Spatial distributions of SOC and nutrient losses

The vegetation and climate have significant impacts on dust emissions (Musick and Gillette, 1990; Hupy, 2004; Peng et al., 2010; Song et al., 2016). The spring NDVI (a vegetation growth indicator) in Northern China significantly increased from 1982 to 1997, but then slightly decreased from 1997 to 2006 (Zhou et al., 2001; Piao et al., 2011). Across the research region, the prescribed NDVI in growing season (April–October), spring, summer, and autumn increased during

1982–1997, whereas decreased from 1997 to 2010 (Fig. S6). Dust emissions and SOC and nutrient losses (Fig. 6) showed negative correlations with NDVI during both the time periods.

The climate change is one of the main drivers of vegetation dynamics (Zhou et al., 2001; Piao et al., 2006b, 2011). Vegetation growth is highly sensitive to temperature changes in boreal and temperate regions at the beginning and end of growing season (Tanja et al., 2003; Piao et al., 2008). Growing season temperatures increased across most intensive wind erosion areas in Northern China from 1982 to 1997, but slightly decreased from 1997 to 2006, which could result in the elevated and declined NDVI during the two periods (Piao et al., 2011), respectively. Moreover, summer precipitation across Inner Mongolia increased during the period 1982–1997 and declined from 1997 to 2006 (Piao et al., 2011), which resulted in the increase and decrease vegetation growth in summer. Vegetation activities in summer contribute primarily to the annual plant growth (Piao et al., 2003; Lee and Sohn, 2011) and could directly influence spring dust emissions in Northern China. Li et al. (2015) reported that the earlier vegetation green-up date has dampening effects on regional spring dust storm frequencies. During the period of 1982–1997, the green-up date of vegetation has advanced in spring by 0.79 days yr^{-1} (Piao et al., 2006a) or 1.3 days per decade (Cong et al., 2013) and the dormancy delayed in autumn by 0.37 days yr^{-1} (Piao et al., 2006a) in Northern China. However, we can capture the delayed green-up date of vegetation after 1997 in Fig. 1 of the multimethod analysis by Cong et al. (2013). The shifts of phenology, therefore, could be another influencing factor that results in the decreased and increased trends of dust emissions before and after 1997.

The spring wind speed across most research areas decreased during the periods of 1982–2011, 1982–1997, and 1997–2011 (Fig. S7). Although wind speed decreased at some meteorological sites (Fig. S7c), the surface friction wind speed would increase due to the reduced surface roughness induced by vegetation cover decreases and result in dust storm breaks. Changes in dust emissions were negatively correlated with changes in the temperature in dust source regions during 1996–1997 and 1997–1998 (Fig. S8a). This may be due to the higher temperatures over all the research region (not shown) in 1997 than that in 1996 and 1998, which could lead to lower wind speeds and result in lower dust emissions in 1997. Although there were no significant correlations between changes in dust emissions and changes in precipitations (Fig. S8b), the precipitations observed in most meteorological sites over dust source regions in 1997 were higher than in 1996 and 1998 (not shown). Moreover, the association of higher temperatures and precipitations in spring could stimulate the vegetation growth and then lead to the lower dust emissions.

4.2. Uncertainties of SOC and nutrient losses

The SOC loss rates by wind erosion for the Earth, United States, and China have been estimated to be as high as 1.4 Pg yr^{-1}, 34 Tg yr^{-1}, and 75 Tg yr^{-1}, respectively (Yan et al., 2005). However, other estimations on the SOC losses in China were 15.9 Tg yr^{-1} (Wen, 1993) and 3 Tg yr^{-1} (Duan et al., 1996), which is 1/5 and 1/25 of the estimation by Yan et al. (2005), respectively. These assessments simply calculated SOC losses by multiplying the wind erosion intensity obtained from remote sensing images and SOC contents in surface soils, which might have large uncertainties in the estimation of the SOC erosion as the assumption of dust emissions are equal from year to year and the selective removal and enrichment of SOC are not accounted for (Webb et al., 2012). In our simulations with the process-based dust emission model using meteorological datasets with high spatial and temporal resolutions, the annual SOC losses in spring was 0.985 ± 0.149 Tg yr^{-1} during 1982–2011 and was similar to the simulation results by Du et al. (2019) (0.808 Tg yr^{-1}, 2001–2014) and Lei et al. (2019) (0.894 Tg yr^{-1}, 1980–2013) in Northern China. Moreover, the SOC emission rate caused by spring wind erosion in this study (0.5 g m^{-2} yr^{-1}) is similar to the 16-year simulation by Chappell et al. (2019) (0.01 t C ha^{-1} yr^{-1}) in Northern China. Dust emissions have large spatial and temporal variations over the past several decades. However, most current estimations of SOC losses were generated by the constant of annual wind erosion intensity directly multiplied the spatial distributions of SOC contents (Yan et al., 2005), which may overestimate the SOC losses due to the large spatial and temporal variations of dust emissions are not considered. Moreover, the SOC and nutrient losses in this study were limited to springtime dust emissions. The SOC losses under spring dust emissions in this study accounted for around 12%–16.2% of the total carbon sequestration of grassland (7 Tg yr^{-1}) (Fang et al., 2007) in Northern China. The omission of SOC losses due to wind erosion from C cycling and C accounting, therefore, is a significant source of uncertainty in C cycle.

The dust emission trend was consistent with the trend of dust storm frequencies in China (Zhang et al., 2003; Wang et al., 2005; Li et al., 2015). In addition, the performance of the dust emission model was evaluated using data from the field investigations and the results revealed that the dust emission model can well simulate dust emission rates in Northern China. The accuracy of the meteorological datasets, which were used in the model, can directly lead to potential errors for the simulations of dust emissions and SOC and nutrient losses. Although the correlation coefficient between the CMFD wind field and observed wind velocity is higher than wind fields of NCEP and ECMWF, the simulations by CMFD could have greater potential errors than other estimations because the CMFD may be generated by interpolation methods, which leads to approximately equal wind speeds between the observed and CMFD at meteorological stations. Changes of climate, land use, and vegetation growth could have significant impacts on soil nutrient dynamics (Cao and Woodward, 1998; McGrath et al., 2001; Ehrenfeld, 2003). However, the SOC and nutrient datasets used in the wind erosion model were held constant in this study. All the SOC and nutrient datasets were generated based on the soil profile data during 1980s. To improve the accuracy of SOC and nutrient losses by wind erosion, it is critical to develop soil nutrient datasets with high spatial and temporal resolutions after 1990s.

Few studies have been conducted to assess the TN and TP losses under wind erosion in China. The magnitudes of spring TN losses by wind erosion in Northern China estimated in this study (Fig. 6c) are consistent with those in a previous study (0.5–9 g N m^{-2} yr^{-1}) (Wang et al., 2006) and 0.184 Tg yr^{-1} (Du et al., 2019). Although we did not evaluate the accuracy of TP dataset adopted in this study, the TP losses (0.089 ± 0.013 Tg yr^{-1}) by spring wind erosion was similar to the simulation results by Du et al. (2019) (0.123 Tg yr^{-1}) and might be, to the best of our knowledge, one of the few assessments in China.

Most eroded soil nutrients were redeposited on the land, rather than in the ocean (Yan and Shi, 2004; Yan et al., 2005). However, this study examined the gross losses of SOC and nutrients from dust emissions, but excluded dust deposition processes and hence neglected the balance of soil nutrient inputs and outputs (net SOC and nutrient redistribution). Our estimations of SOC and nutrient losses by wind erosion were based on the assumption that the SOC and nutrient contents of eroded material were the same as those of the surface soils. However, Webb et al. (2012) reported that the measured SOC content of Australian dusts can be up to seven times higher than that of parent soils, with enrichment factors ranged from 1.67 to 7.09. All the mentioned impacting factors can result in potential uncertainties in the estimates of SOC and nutrient losses by wind erosion. To reduce the uncertainty in SOC and nutrient losses under wind erosion, it is critical to improve the accuracy of dust budgets simulations, to develop soil nutrient datasets with high spatial and temporal resolutions, and to compare SOC, TN, and TP contents in emission dusts with those in parent soils in China.

4.3. Implications for SOC and nutrient losses

Across the whole earth, 65% of the annual global dust emissions (Miller et al., 2004) are from North Africa and 25% from Asia (Ginoux et al., 2004) and 75% of which are deposited on the land and 25% in the ocean (Shao et al., 2011). Wind erosion is one of the major processes in influencing SOC and nutrient budgets in Northern China. In China, approximately 800 Tg of desert dusts are injected into the atmosphere annually and 30% of it are redeposited to the deserts, 20% are deposited to the downwind terrestrial ecosystems and fresh water of China, and the remaining 50% of the dusts are subject to long-range transport to the Pacific Ocean and beyond (Zhang et al., 1997). Strong dust emissions resulted from wind erosion can cause severe soil degradation and inhibit primary productivity in the source region due to the losses of SOC and nutrients (Bielders et al., 2002; Hoffmann et al., 2011; Labiadh et al., 2013). Dust supply associated with SOC and nutrients can directly affect primary production, species composition, C cycle, and N fixation in terrestrial and aquatic (fresh water and ocean) ecosystems and will affect local and global biogeochemistry (Jickells et al., 2005; Mahowald et al., 2005; Maher et al., 2010). Research is required to explore the impacts of dust transport and deposition processes on productivity and biogeochemical cycles from dust resource regions to local, regional, and global scales.

5. Conclusions

This study simulated the spatial and temporal dynamics of SOC, TN, and TP losses under spring wind erosion in Northern China forced by three types of wind field datasets of NCEP, ECMWF, and CMFD during the period 1982–2011. Comprehensive assessments on the losses of SOC, TN, and TP caused by spring wind erosion in arid and semi-arid regions of Northern China are conducted based on the data from the field investigations that directly mimiking wind erosion.

At the regional scale, temporal trends in losses of SOC, TN, and TP are consistent with dust emissions from 1982 to 2011. The average of spring dust emissions is $154.45 \pm 21.28\,\mathrm{Tg\,yr^{-1}}$ and the annual losses of SOC, TN, and TP during spring are $0.985 \pm 0.149\,\mathrm{Tg\,yr^{-1}}$, $0.094 \pm 0.014\,\mathrm{Tg\,yr^{-1}}$, and $0.089 \pm 0.013\,\mathrm{Tg\,yr^{-1}}$, respectively. Two distinct periods with opposite trends before and after 1997 are identified in SOC and nutrient losses in Northern China. Dust emissions mainly occur in areas with low SOC contents in the top soils. Areas of severe losses of SOC, TN, and TP mainly distribute in Western Inner Mongolia, Western Gansu, Northern Qinghai, and Eastern Xinjiang. Elevated and declined NDVI resulted from increased and decreased temperatures and summer precipitation in growing seasons could lead to the two periods with opposite trends in SOC and nutrient losses.

Although numerous impacting factors can cause potential uncertainty in estimating SOC and nutrient losses by wind erosion, very little is known concerning the linkages between dust processes and the productivity and biogeochemical cycles of terrestrial ecosystems. Losses of SOC and nutrients by wind erosion in Northern China should be included in projecting plant growth and ecosystem productivity, especially in dust storm-prone areas. It is critical to reduce the uncertainties in simulating regional biogeochemical cycling.

Declaration of interests

The authors declare that they have no known competing financial interests or personal relationships that could have appeared to influence the work reported in this paper.

Acknowledgments

This study was financially supported by the National Natural Science Foundation of China (31430015, 31830012, and 41401107). We the authors thank Shufei Song from University of Pennsylvania for help in improving the language, Ang Zhang, Jingyi Ru, Mingxing Zhong, Zhenxing Zhou, Mengyang Yu, Mouyao Xiao, Yuan Miao, and Bin Liu help in the field experiments. The HWSD data were obtained from the FAO SOILS PORTAL (http://www.fao.org/soils-portal/soil-survey/soil-maps-and-databases/harmonized-world-soil-database-v12/en/). The NDVI3g data were generated by AVHRR and can be directly downloaded from NASA (https://ecocast.arc.nasa.gov/data/pub/gimms). The land use data were obtained from the Data Sharing Infrastructure of Earth System Science (http://www.geodata.cn). The wind field datasets of NCEP and CMFD can be accessed on NOAA (https://www.esrl.noaa.gov/psd/data/gridded/data.ncep.reanalysis.html) and WestDC (http://westdc.westgis.ac.cn/data/7a35329c-c53f-4267-aa07-e0037d913a21), respectively. Model outputs and observations of SOC and TN are freely available at http://www.3sgeo.cn/data/jgr_bio_2017.

Appendix A. Supplementary data

Supplementary data to this article can be found online at https://doi.org/10.1016/j.atmosenv.2019.06.043.

References

Bielders, C.L., Rajot, J.L., Amadou, M., 2002. Transport of soil and nutrients by wind in bush fallow land and traditionally managed cultivated fields in the Sahel. Geoderma 109, 19–39. https://doi.org/10.1016/S0016-7061(02)00138-6.

Cao, M., Woodward, F.I., 1998. Dynamic responses of terrestrial ecosystem carbon cycling to global climate change. Nature 393, 249–252. https://doi.org/10.1038/30460.

Cao, S., Chen, L., Shankman, D., Wang, C., Wang, X., Zhang, H., 2011. Excessive reliance on afforestation in China's arid and semi-arid regions: lessons in ecological restoration. Earth Sci. Rev. 104, 240–245. https://doi.org/10.1016/j.earscirev.2010.11.002.

Chappell, A., Webb, N.P., Butler, H.J., Strong, C.L., McTainsh, G.H., Leys, J.F., Viscarra Rossel, R.A., 2013. Soil organic carbon dust emission: an omitted global source of atmospheric CO_2. Glob. Chang. Biol. 19, 3238–3244. https://doi.org/10.1111/gcb.12305.

Chappell, A., Webb, N.P., Leys, J., Waters, C.M., Orgill, S., Eyres, M., 2019. Minimising soil organic carbon erosion by wind is critical for land degradation neutrality. Environ. Sci. Policy 93, 43–52.

Chappell, A., Webb, N.P., Rossel, R.V., Bui, E., 2014. Australian net (1950s–1990) soil organic carbon erosion: implications for CO_2 emission and land-atmosphere modelling. Biogeosciences 11, 5235–5244. https://doi.org/10.5194/bg-11-5235-2014.

Cong, N., Wang, T., Nan, H., Ma, Y., Wang, X., Myneni, R.B., Piao, S., 2013. Changes in satellite-derived spring vegetation green-up date and its linkage to climate in China from 1982 to 2010: a multimethod analysis. Glob. Chang. Biol. 19, 881–891. https://doi.org/10.1111/gcb.12077.

Cowie, S.M., Knippertz, P., Marsham, J.H., 2013. Are vegetation-related roughness changes the cause of the recent decrease in dust emission from the Sahel? Geophys. Res. Lett. 40, 1868–1872. https://doi.org/10.1002/grl.50273.

Du, H., Wang, T., Xue, X., Li, S., 2019. Estimation of soil organic carbon, nitrogen, and phosphorus losses induced by wind erosion in northern China. Land Degrad. Dev. 30, 1006–1022.

Du, H., Xue, X., Wang, T., 2014. Estimation of the quantity of aeolian saltation sediments blown into the Yellow River from the Ulanbuh Desert, China. J. Arid. Land 6, 205–218. https://doi.org/10.1007/s40333-013-0198-3.

Duan, Z., Liu, X., Qu, J., 1996. Influences of land desertification to atmosphere in China. Res. Environ. Arid Region 10 (2), 89–93 (in Chinese with English abstract).

Ehrenfeld, J.G., 2003. Effects of exotic plant invasions on soil nutrient cycling processes. Ecosystems 6, 503–523. https://doi.org/10.1007/s10021-002-0151-3.

Evan, A.T., Flamant, C., Gaetani, M., Guichard, F., 2016. The past, present and future of African dust. Nature 531, 493–495. https://doi.org/10.1038/nature17149.

Fang, J.Y., Guo, Z.D., Piao, S.L., Chen, A., 2007. Terrestrial vegetation carbon sinks in China, 1981-2000. Sci. China, Ser. A D 50, 1341–1350. https://doi.org/10.1007/s11430-007-0049-1.

Ginoux, P., Deroubaix, A., 2017. Space observations of dust in East Asia. In: Air Pollution in Eastern Asia: an Integrated Perspective. Springer, Cham, pp. 365–383. https://link.springer.com/chapter/10.1007%2F978-3-319-59489-7_17.

Ginoux, P., Prospero, J.M., Torres, O., Chin, M., 2004. Long-term simulation of global dust distribution with the GOCART model: correlation with North Atlantic Oscillation. Environ. Model. Softw 19, 113–128. https://doi.org/10.1016/S1364-8152(03)00114-2.

Griffin, D.W., 2007. Atmospheric movement of microorganisms in clouds of desert dust and implications for human health. Clin. Microbiol. Rev. 20, 459–477. https://doi.org/10.1128/CMR.00039-06.

Grousset, F.E., Ginoux, P., Bory, A., Biscaye, P.E., 2003. Case study of a Chinese dust plume reaching the French Alps. Geophys. Res. Lett. 30 (6) 10-11-10-4. https://doi.org/10.1029/2002GL016833.

Harper, R.J., Gilkes, R.J., Hill, M.J., Carter, D.J., 2010. Wind erosion and soil carbon dynamics in south-western Australia. Aeolian Res 1, 129–141. https://doi.org/10.1016/j.aeolia.2009.10.003.

He, J., Yang, K., 2011. China meteorological forcing dataset. Cold and arid regions science data center at lanzhou. https://doi.org/10.3972/westdc.002.2014.db.

Hoffmann, C., Funk, R., Reiche, M., Li, Y., 2011. Assessment of extreme wind erosion and its impacts in Inner Mongolia, China. Aeolian Res 3, 343–351. https://doi.org/10.1016/j.aeolia.2011.07.007.

Huneeus, N., Schulz, M., Balkanski, Y., Griesfeller, J., Prospero, M.J., Kinne, S., Bauer, S., Boucher, O., Chin, M., Dentener, F., Diehl, T., Easter, R., Fillmore, D., Ghan, S., Ginoux, P., Grini, A., Horowitz, L., Koch, D., Krol, M.C., Landing, W., Liu, X., Mahowald, N., Miller, R., Morecrette, J.-J., Myhre, G., Penner, J., Perlwitz, J., Stier, P., Takemura, T., Zender, C.S., 2011. Global dust model intercomparison in AeroCom phase I. Atmos. Chem. Phys. 11, 7781–7816. https://doi.org/10.5194/acp-11-7781-2011.

Hupy, J.P., 2004. Influence of vegetation cover and crust type on wind-blown sediment in a semi-arid climate. J. Arid Environ. 58, 167–179. https://doi.org/10.1016/S0140-1963(03)00129-0.

Jickells, T.D., An, Z.S., Andersen, K.K., Baker, A.R., Bergametti, G., Brooks, N., Cao, J.J., Boyd, P.W., Duce, R.A., Hunter, K.A., Kawahata, H., 2005. Global iron connections between desert dust, ocean biogeochemistry, and climate. Science 308, 67–71. https://doi.org/10.1126/science.1105959.

Katra, I., Gross, A., Swet, N., Tanner, S., Krasnov, H., Angert, A., 2016. Substantial dust loss of bioavailable phosphorus from agricultural soils. Sci. Rep. 6, 24736. https://doi.org/10.1038/srep24736.

Kim, H., Choi, M., 2015. Impact of soil moisture on dust outbreaks in East Asia: using satellite and assimilation data. Geophys. Res. Lett. 42, 2789–2796. https://doi.org/10.1002/2015GL063325.

Labiadh, M., Bergametti, G., Kardous, M., Perrier, S., Grand, N., Attoui, B., Sekrafi, S., Marticorena, B., 2013. Soil erosion by wind over tilled surfaces in South Tunisia. Geoderma 202, 8–17. https://doi.org/10.1016/j.geoderma.2013.03.007.

Lee, E.H., Sohn, B.J., 2011. Recent increasing trend in dust frequency over Mongolia and Inner Mongolia regions and its association with climate and surface condition change. Atmos. Environ. 45, 4611–4616. https://doi.org/10.1016/j.atmosenv.2011.05.065.

Lei, L., Zhang, K., Zhang, X., Wang, Y.P., Xia, J., Piao, S., Hui, D., Zhong, M., Ru, J., Zhou, Z., Song, H., Yang, Z., Wang, D., Miao, Y., Yang, F., Liu, B., Zhang, A., Yu, M., Liu, X., Song, Y., Zhu, L., Wan, S., 2019. Plant feedback aggravates soil organic carbon loss associated with wind erosion in Northwest China. J. Geophys. Res.-Biogeo 124, 825–839. https://doi.org/10.1029/2018JG004804.

Lelieveld, J., Evans, J.S., Fnais, M., Giannadaki, D., Pozzer, A., 2015. The contribution of outdoor air pollution sources to premature mortality on a global scale. Nature 525, 367–371. https://doi.org/10.1038/nature15371.

Li, N., Guo, L., Fan, B., 2015. A new perspective on understanding the reduced spring dust storm frequency in Inner Mongolia, China. Int. J. Disaster Risk Sci. 6, 216–225. https://doi.org/10.1007/s13753-015-0062-5.

Li, X., Song, H., Zhai, S., Lu, S., Kong, Y., Xia, H., Zhao, H., 2019. Particulate matter pollution in Chinese cities: areal-temporal variations and their relationships with meteorological conditions (2015–2017). Environ. Pollut. 246, 11–18. https://doi.org/10.1016/j.envpol.2018.11.103.

Liu, X., Yin, Z.Y., Zhang, X., Yang, X., 2004. Analyses of the spring dust storm frequency of northern China in relation to antecedent and concurrent wind, precipitation, vegetation, and soil moisture conditions. J. Geophys. Res.-Atmos. 109, D16210. https://doi.org/10.1029/2004JD004615.

Lu, H., Shao, Y., 2001. Toward quantitative prediction of dust storms: an integrated wind erosion modelling system and its applications. Environ. Model. Softw 16, 233–249. https://doi.org/10.1016/S1364-8152(00)00083-9.

Lu, H., Shao, Y., 1999. A new model for dust emission by saltation bombardment. J. Geophys. Res.-Atmos. 104, 16827–16842. https://doi.org/10.1029/1999JD900169.

Maher, B.A., Prospero, J.M., Mackie, D., Gaiero, D., Hesse, P.P., Balkanski, Y., 2010. Global connections between aeolian dust, climate and ocean biogeochemistry at the present day and at the last glacial maximum. Earth Sci. Rev. 99, 61–97. https://doi.org/10.1016/j.earscirev.2009.12.001.

Mahowald, N.M., Baker, A.R., Bergametti, G., Brooks, N., Duce, R.A., Jickells, T.D., Kubilay, N., Prospero, J.M., Tegen, I., 2005. Atmospheric global dust cycle and iron inputs to the ocean. Glob. Biogeochem. Cycles 19, GB4025. https://doi.org/10.1029/2004GB002402.

Mao, R., Ho, C.H., Feng, S., Gong, D.Y., Shao, Y., 2013. The influence of vegetation variation on Northeast Asian dust activity. Asia Pac. J. Atmos. Sci. 49, 87–94. https://doi.org/10.1007/s13143-013-0010-5.

Mao, R., Ho, C.H., Shao, Y., Gong, D.Y., Kim, J., 2011. Influence of arctic oscillation on dust activity over northeast Asia. Atmos. Environ. 45, 326–337. https://doi.org/10.1016/j.atmosenv.2010.10.020.

McGrath, D.A., Smith, C.K., Gholz, H.L., Oliveira, F.D.A., 2001. Effects of land-use change on soil nutrient dynamics in Amazonia. Ecosystems 4, 625–645. https://doi.org/10.1007/s10021-001-0033-0.

Miller, R.L., Tegen, I., Perlwitz, J., 2004. Surface radiative forcing by soil dust aerosols and the hydrologic cycle. J. Geophys. Res.-Atmos. 109, D04203. https://doi.org/10.1029/2003JD004085.

Monks, P.S., Granier, C., Fuzzi, S., Stohl, A., Williams, M.L., Akimoto, H., Amann, M., Baklanov, A., Baltensperger, U., Bey, I., Blake, N., Blake, R.S., Carslaw, K., Cooper, O.R., Dentener, F., Fowler, D., Fragkou, E., Frost, G.J., Generoso, S., Ginoux, P., Grewe, V., Guenther, A., Hansson, H.C., Henne, S., Hjorth, J., Hofzumahaus, A., Huntriese, r H., Isaksen, I.S.A., Jenkin, M.E., Kaiser, J., Kanakidou, M., Klimont, Z., Kulmala, M., Laj, P., Lawrence, M.G., Lee, J.D., Liousse, C., Maione, M., McFiggans, G., Metzger, A., Mieville, A., Moussiopoulos, N., Orlando, J.J., O'Dowd, C.D., Palmer, P.I., Parrish, D.D., Petzold, A., Platt, U., Pöschl, U., Prévôt, A.S.H., Reeves, C.E., Reimann, S., Rudich, Y., Sellegri, K., Steinbrecher, R., Simpson, D., ten Brink, H., Theloke, J., van der Werf, G.R., Vautard, R., Vestreng, V., Vlachokostas, Ch, von Glasow, R., 2009. Atmospheric composition change–global and regional air quality. Atmos. Environ. 43, 5268–5350. https://doi.org/10.1016/j.atmosenv.2009.08.021.

Musick, H.B., Gillette, D.A., 1990. Field evaluation of relationships between a vegetation structural parameter and sheltering against wind erosion. Land Degrad. Dev. 2, 87–94. https://doi.org/10.1002/ldr.3400020203.

Owen, R.P., 1964. Saltation of uniform grains in air. J. Fluid Mech 20, 225–242. https://doi.org/10.1017/S0022112064001173.

Peng, S., Piao, S., Ciais, P., Fang, J., Wang, X., 2010. Change in winter snow depth and its impacts on vegetation in China. Glob. Chang. Biol. 16, 3004–3013. https://doi.org/10.1111/j.1365-2486.2010.02210.x.

Piao, S., Ciais, P., Friedlingstein, P., Peylin, P., Reichstein, M., Luyssaert, S., Margolis, H., Fang, J., Barr, A., Chen, A., Grelle, A., 2008. Net carbon dioxide losses of northern ecosystems in response to autumn warming. Nature 451, 49–53. https://doi.org/10.1038/nature06444.

Piao, S., Fang, J., Zhou, L., Ciais, P., Zhu, B., 2006a. Variations in satellite-derived phenology in China's temperate vegetation. Glob. Chang. Biol. 12, 672–685. https://doi.org/10.1111/j.1365-2486.2006.01123.x.

Piao, S., Fang, J., Zhou, L., Guo, Q., Henderson, M., Ji, W., Li, Y., Tao, S., 2003. Interannual variations of monthly and seasonal normalized difference vegetation index (NDVI) in China from 1982 to 1999. J. Geophys. Res.-Atmos. 108, 4401. https://doi.org/10.1029/2002JD002848.

Piao, S., Friedlingstein, P., Ciais, P., Zhou, L., Chen, A., 2006b. Effect of climate and CO_2 changes on the greening of the Northern Hemisphere over the past two decades. Geophys. Res. Lett. 33, L23402. https://doi.org/10.1029/2006GL028205.

Piao, S., Wang, X., Ciais, P., Zhu, B., Wang, T.A.O., Liu, J.I.E., 2011. Changes in satellite-derived vegetation growth trend in temperate and boreal Eurasia from 1982 to 2006. Glob. Chang. Biol. 17, 3228–3239. https://doi.org/10.1111/j.1365-2486.2011.02419.x.

Raupach, M.R., Gillette, D.A., Leys, J.F., 1993. The effect of roughness elements on wind erosion threshold. J. Geophys. Res.-Atmos. 98, 3023–3029. https://doi.org/10.1029/92JD01922.

Reynolds, R., Belnap, J., Reheis, M., Lamothe, P., Luiszer, F., 2001. Aeolian dust in Colorado Plateau soils: nutrient inputs and recent change in source. P. Natl. Acad. Sci. USA 98, 7123–7127. https://doi.org/10.1073/pnas.121094298.

Shangguan, W., Dai, Y., Liu, B., Zhu, A., Duan, Q., Wu, L., Ji, D., Ye, A., Yuan, H., Zhang, Q., Chen, D., 2013. A China data set of soil properties for land surface modeling. J. Adv. Model. Earth Syst. 5, 212–224. https://doi.org/10.1002/jame.20026.

Shao, Y., Jung, E., Leslie, L.M., 2002. Numerical prediction of northeast Asian dust storms using an integrated wind erosion modeling system. J. Geophys. Res.-Atmos. 107 (D24) AAC 21-1-AAC 21-23. https://doi.org/10.1029/2001JD001493.

Shao, Y., Wyrwoll, K.H., Chappell, A., Huang, J., Lin, Z., McTainsh, G.H., Mikami, M., Tanaka, T.Y., Wang, X., Yoon, S., 2011. Dust cycle: an emerging core theme in Earth system science. Aeolian Research 2, 181–204. https://doi.org/10.1016/j.aeolia.2011.02.001.

Shao, Y., Yang, Y., Wang, J., Song, Z., Leslie, L.M., Dong, C., Zhang, Z., Lin, Z., Kanai, Y., Yabuki, S., Chun, Y., 2003. Northeast Asian dust storms: real-time numerical prediction and validation. J. Geophys. Res.-Atmos. 108 (D22) AAC-3. https://doi.org/10.1029/2003JD003667.

Shi, X.Z., Yu, D.S., Warner, E.D., Pan, X.Z., Petersen, G.W., Gong, Z.G., Weindorf, D.C., 2004. Soil database of 1: 1,000,000 digital soil survey and reference system of the Chinese genetic soil classification system. Soil Horiz. 45, 129–136. https://doi.org/10.2136/sh2004.4.0129.

Song, H., Wang, K., Zhang, Y., Hong, C., Zhou, S., 2017. Simulation and evaluation of dust emissions with WRF-Chem (v3. 7.1) and its relationship to the changing climate over East Asia from 1980 to 2015. Atmos. Environ. 167, 511–522. https://doi.org/10.1016/j.atmosenv.2017.08.051.

Song, H., Zhang, K., Piao, S., Wan, S., 2016. Spatial and temporal variations of spring dust emissions in northern China over the last 30 years. Atmos. Environ. 126, 117–127. https://doi.org/10.1016/j.atmosenv.2015.11.052.

Su, L., Fung, J.C., 2015. Sensitivities of WRF-Chem to dust emission schemes and land surface properties in simulating dust cycles during springtime over East Asia. J. Geophys. Res.-Atmos 120, 11215–11230. https://doi.org/10.1002/2015JD023446.

Tanja, S., Berninger, F., Vesala, T., Markkanen, T., Hari, P., Makela, A., Ilvesniemi, H., Hanninen, H., Nikinmaa, E., Huttula, T., Laurila, T., Aurela, M., Grelle, A., Lindroth, A., Arneth, A., Shibistova, O., Lloyd, J., 2003. Air temperature triggers the recovery of evergreen boreal forest photosynthesis in spring. Glob. Chang. Biol. 9, 1410–1426. https://doi.org/10.1046/j.1365-2486.2003.00597.x.

Tegen, I., Lacis, A.A., Fung, I., 1996. The influence on climate forcing of mineral aerosols from disturbed soils. Nature 380, 419. https://doi.org/10.1038/380419a0.

Tucker, C.J., Pinzon, J.E., Brown, M.E., Slayback, D.A., Pak, E.W., Mahoney, R., Vermote, E.F., El Saleous, N., 2005. An extended AVHRR 8-km NDVI dataset compatible with MODIS and SPOT vegetation NDVI data. Int. J. Remote Sens. 26, 4485–4498. https://doi.org/10.1080/01431160500168686.

Van Oost, K., Quine, T.A., Govers, G., De Gryze, S., Six, J., Harden, J.W., Ritchie, J.C., McCarty, G.W., Heckrath, G., Kosmas, C., Giraldez, J.V., 2007. The impact of agricultural soil erosion on the global carbon cycle. Science 318, 626–629. https://doi.org/10.1126/science.1145724.

Wang, S., Wang, J., Zhou, Z., Shang, K., 2005. Regional characteristics of three kinds of dust storm events in China. Atmos. Environ. 39, 509–520. https://doi.org/10.1016/j.atmosenv.2004.09.033.

Wang, X., Oenema, O., Hoogmoed, W.B., Perdok, U.D., Cai, D., 2006. Dust storm erosion and its impact on soil carbon and nitrogen losses in northern China. Catena 66, 221–227. https://doi.org/10.1016/j.catena.2006.02.006.

Webb, N.P., Chappell, A., Strong, C.L., Marx, S.K., McTainsh, G.H., 2012. The significance of carbon-enriched dust for global carbon accounting. Glob. Chang. Biol. 18, 3275–3278. https://doi.org/10.1111/j.1365-2486.2012.02780.x.

Wen, D., 1993. Soil erosion and conservation in China. In: Pimentel, D. (Ed.), World Soil Erosion and Conservation. Cambridge University Press, Cambridge, UK, pp. 63–86.

Yan, H., Wang, S., Wang, C., Zhang, G., Patel, N., 2005. Losses of soil organic carbon under wind erosion in China. Glob. Chang. Biol. 11, 828–840. https://doi.org/10.1111/j.1365-2486.2005.00950.x.

Yan, P., Shi, P., 2004. Using the ^{137}Cs technique to estimate wind erosion in gonghe basin, Qinghai province, China. Soil Sci. 169, 295–305. https://doi.org/10.1097/01.ss.0000126843.88716.d3.

Yu, H., Chin, M., Yuan, T., Bian, H., Remer, L.A., Prospero, J.M., Omar, A., Winker, D., Yang, Y., Zhang, Y., Zhang, Z., 2015. The fertilizing role of African dust in the Amazon rainforest: a first multiyear assessment based on data from Cloud-Aerosol Lidar and Infrared Pathfinder Satellite Observations. Geophys. Res. Lett. 42, 1984–1991. https://doi.org/10.1002/2015GL063040.

Yu, H., Remer, L.A., Chin, M., Bian, H., Tan, Q., Yuan, T., Zhang, Y., 2012. Aerosols from overseas rival domestic emissions over North America. Science 337, 566–569. https://doi.org/10.1126/science.1217576.

Zhang, X.Y., Arimoto, R., An, Z.S., 1997. Dust emission from Chinese desert sources linked to variations in atmospheric circulation. J. Geophys. Res.-Atmos. 102, 28041–28047. https://doi.org/10.1029/97JD02300.

Zhang, X.Y., Gong, S.L., Zhao, T.L., Arimoto, R., Wang, Y.Q., Zhou, Z.J., 2003. Sources of Asian dust and role of climate change versus desertification in Asian dust emission. Geophys. Res. Lett. 30, 2272. https://doi.org/10.1029/2003GL018206.

Zhou, L., Tucker, C.J., Kaufmann, R.K., Slayback, D., Shabanov, N.V., Myneni, R.B., 2001. Variations in northern vegetation activity inferred from satellite data of vegetation index during 1981 to 1999. J. Geophys. Res.-Atmos. 106, 20069–20083. https://doi.org/10.1029/2000JD000115.